journal

J. Am. Ceram. Soc., 95 [1] 232–237 (2012)
DOI: 10.1111/j.1551-2916.2011.04760.x

Microwave and Infrared Dielectric Response of Temperature Stable $(1-x)BaMoO_4$–$xTiO_2$ Composite Ceramics

Jing Guo,[‡,§] Di Zhou,[‡,§] Hong Wang,[‡,§,†] Yuehua Chen,[‡,§] Yi Zeng,[‡,§] Feng Xiang,[‡,§] Ying Wu,[‡,§] and Xi Yao[‡,§]

[‡]Electronic Materials Research Laboratory, Key Laboratory of the Ministry of Education, Xi'an Jiaotong University, Xi'an, 710049, China

[§]International Center for Dielectric Research, Xi'an Jiaotong University, Xi'an, 710049, China

The $(1-x)BaMoO_4$–$xTiO_2$ (x = 0.0, 0.2, 0.3, 0.338, 0.4, 0.5, 0.66) ceramics were synthesized by the conventional mixed-oxide process. The sintering behaviors, phase composition, chemical compatibility with silver, and microwave dielectric properties of pure $(1-x)BaMoO_4$–$xTiO_2$ ceramics and $0.662BaMoO_4$–$0.338TiO_2$ ceramic with H_3BO_3–CuO addition were studied. Infrared reflectivity spectra of $(1-x)BaMoO_4$–x TiO_2 ($0.2 \leq x \leq 0.4$) composites were measured in the range of 50–4500 cm^{-1} at room temperature. X-ray diffraction analysis reveals that scheelite $BaMoO_4$ and rutile TiO_2 phase coexist with each other at 1275°C and both of them do not react with silver (Ag) at 850°C. When the mole fraction of TiO_2 (x value) is 0.4, a temperature stable microwave dielectric material is obtained, with ε_r = 13.8, $Q \times f$ = 40 500 GHz (f = 8.02 G), and τ_f = −6.13 ppm/°C. Complex dielectric spectra gained from the infrared spectra were extrapolated down to microwave range, and they were in good agreement with the measured microwave permittivity and dielectric losses. With 5 wt% H_3BO_3 and 1 wt% CuO addition, the 0.662 $BaMoO_4$–$0.338TiO_2$ ceramics can be sintered well below 900°C, and possess good microwave dielectric properties with ε_r = 14, $Q \times f$ = 48 360 GHz, and τ_f = +13.9 ppm/°C.

I. Introduction

With the development of high-frequency wireless communication technology, low temperature cofired ceramic (LTCC) technology, which can integrate the passive components to a function module, has attracted much scientific and commercial attention. For microwave (MW) applications, dielectric materials should have a low sintering temperature, a high quality factor ($Q \times f$) value, a near-zero temperature coefficient of resonant frequency (τ_f), and chemical compatibility with metal electrodes.[1–5] Recently, MW dielectric properties of $AMoO_4$ ceramics with scheelite (A = Ca, Sr, Ba) and wolframite (A = Mg, Mn, Zn) structure have been reported.[6–8] All of them exhibit good MW dielectric properties (permittivity ε_r = 7–11, $Q \times f$ = 37 000–90 000 GHz, τ_f = −57 to −87 ppm/°C). The $BaMoO_4$ has the largest negative τ_f value (−79.24 ppm/°C) and the lowest sintering temperature (900°C/2 h) in the series of $AMoO_4$ ceramics with scheelite structure. Therefore, it is interesting to compensate the τ_f value of $BaMoO_4$ using ceramics with large positive τ_f values. Many successful examples have been achieved by mixing two or more materials with opposite τ_f values, such as $Zn_2Te_3O_8$–TiO_2, $(Mg_{0.95}Zn_{0.05})TiO_3$–$SrTiO_3$, $MgTiO_3$–$ZnAl_2O_4$–TiO_2, $Mg_4Nb_2O_9$–$ZnAl_2O_4$–TiO_2, $ZnNb_2O_6$–TiO_2, Mg_2TiO_4–Co_2TiO_4–$CaTiO_3$, $CaWO_4$–TiO_2, and Bi_2MoO_6–TiO_2.[9–15] Our previous study on $ZnMoO_4$–TiO_2 system also demonstrated that the rutile TiO_2 (ε_r = 105, $Q \times f$ = 46 000 GHz, τ_f = +465 ppm/°C) is an effective material to compensate the negative τ_f value of $ZnMoO_4$, which is also a MoO_3-rich compound similar to $BaMoO_4$ but with a wolframite structure.[16] For this reason, rutile TiO_2 is chosen to mix with $BaMoO_4$ as a compensator.

Dielectric losses include intrinsic part and extrinsic part. Intrinsic losses are determined by polar optical phonons and extrinsic losses are caused by impurity, pores, size and shapes of grains, etc. Wakino *et al.*[17] and Tamura *et al.*[18] have reported the relation between intrinsic loss and infrared (IR) spectra. A large amount of research on IR reflective spectra of rutile TiO_2 was done.[19–21] But the investigation on IR spectra of $BaMoO_4$ was few and the complex dielectric response was not discussed.[22–24] Therefore, it is important to study the intrinsic losses of $(1-x)BaMoO_4$–$xTiO_2$ compounds from the infrared spectra and it helps to understand the dielectric loss at microwave region.

In this work, the sintering behaviors, phase composition, chemical compatibility with silver, microwave dielectric properties, and complex dielectric response between 50 and 4500 cm^{-1} of the $(1-x)BaMoO_4$–$xTiO_2$ ceramics were studied. To lower the sintering temperature, H_3BO_3–CuO was added to the composites and its influence on the compounds was also investigated.

II. Experimental Procedure

The $(1-x)BaMoO_4$–$xTiO_2$ composite ceramics were prepared by the conventional solid-state synthesis. Reagent-grade powders $BaCO_3$ (>99%, Sinopharm Chemical Reagent Co. Ltd, Shanghai, China), MoO_3 (>99%, Fuchen Chemical Reagents, Tianjin, China), rutile TiO_2 (>99%, Linghua Co. Ltd., Zhaoqing, China), H_3BO_3 (>99.5%, Sinopharm Chemical Reagent Co. Ltd), and CuO (>99%, Sinopharm Chemical Reagent Co. Ltd) were used as starting materials. The $BaCO_3$ and MoO_3 powders were milled with ethanol and ZrO_2 milling media (2 mm in diameter) for 4 h using a planetary ball-mill. After being dried, the mixture was calcined in air at 650°C for 4 h. Then, some $BaMoO_4$ powder was mixed with TiO_2 according to the following formula $(1-x)$ $BaMoO_4$–$xTiO_2$ ($0 \leq x \leq 0.66$). Furthermore, the other powders were mixed with TiO_2, 5 wt% H_3BO_3, and 1 wt% CuO. The mixture was milled with zirconia balls in ethanol for 4 h and then dried. After being mixed with PVA binder,

D. W. Johnson Jr—contributing editor

Manuscript No. 29623. Received April 20, 2011; approved June 21, 2011.
This work was supported by the National 973-project of China (2009CB623302), NSFC projects of China (61025002, 109790365), and National Project of International Science and Technology Collaboration (2009DFA51820).
[†]Author to whom correspondence should be addressed. e-mail: hwang@mail.xjtu.edu.cn

the final powders were pressed into cylindrical disks (12 mm in diameter and 5–6mm in height) using uniaxial pressing. For $(1-x)BaMoO_4$–$xTiO_2$ and samples with H_3BO_3–CuO addition, pellets were sintered at 1150°C–1300°C and 700°C–900°C for 2 h with a heating rate of 3°C/min, respectively. Chemical compatibility tests with silver were performed by adding 20 wt% Ag to $(1-x)BaMoO_4$–$xTiO_2$ composite with H_3BO_3–CuO addition.

The phase compositions of samples were identified by X-ray diffraction with Cu$K\alpha$ radiation (Rigaku D/MAX-2400 X-ray diffractometry, Tokyo, Japan). A scanning electron microscope (JSM-6460, JEOL, Tokyo, Japan) was used to examine the microstructures of the surfaces. The bulk densities of the composites were determined by Archimedes' method. The dielectric constant and quality factor at microwave frequency were measured using the $TE_{01\delta}$-shielded cavity method with a network analyzer (8720ES, Agilent, Palo Alto, CA). The TCF (τ_f) value was measured in the temperature range of 25°C–85°C, and was calculated as

$$\tau_f = \frac{f_{85} - f_{25}}{f_{25}(85-25)} \times 10^6 (\text{ppm})/^\circ\text{C} \quad (1)$$

where, f_{25} and f_{85} were the resonant frequencies at 25°C and 85°C, respectively. The IR reflectivity spectra were measured between 50 and 4500 cm^{-1} (This measurement was done in the IR beamline of NSRL), by a Fourier transform IR (FTIR) spectrometer (IFS 66v/S Vacuum, Bruker Optik Gmbh, Germany).

III. Results and Discussions

Figure 1 presents the XRD patterns of calcined $BaMoO_4$ powders, $(1-x)BaMoO_4$–$xTiO_2$ composites with various values of x sintered at 1275°C/2 h, specimens with H_3BO_3–CuO addition sintered at 850°C/2 h, and samples cofired with 20 wt% Ag sintered at 850°C/2 h. The pure scheelite $BaMoO_4$ phase was formed at 650°C for 4 h. No secondary phase can be observed when x varies from 0 to 0.66 and the intensity of the diffraction peaks of TiO_2 rises with x value. Hence, it can be concluded that scheelite $BaMoO_4$ phase coexists with rutile TiO_2 phase below 1300°C. The addition of 5 wt% H_3BO_3 and 1 wt% CuO do not bring significant influence on the phase composition and the silver seems not to react with $(1-x)BaMoO_4$–$xTiO_2$ composites.

Figure 2 shows the backscattered electron images (BEI) of the as-fired surfaces of $0.6BaMoO_4$–$0.4TiO_2$ compounds

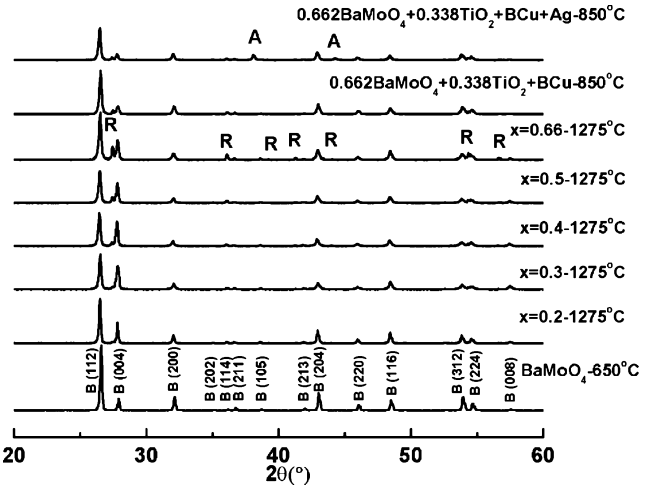

Fig. 1. XRD results of calcined $BaMoO_4$ powder, $(1-x)BaMoO_4$–x TiO_2 ceramics sintering at 1275°C/2 h, specimens with H_3BO_3–CuO addition sintered at 850°C/2 h, and samples cofired with 20 wt% Ag sintered at 850°C/2 h (R, rutile TiO_2; B, $BaMoO_4$; A, Ag).

sintered at 1250°C/2 h, samples with H_3BO_3–CuO addition, and cofired samples with 20 wt% Ag, sintered at 850°C/2 h. It is observed from Fig. 2(a) that two types of grains with different shapes coexist. From the EDS analysis, in Fig. 2(b), it can be found that the light-color grains with polygonal shape marked as A belong to $BaMoO_4$ phase and the dark-color ones with bar shape marked as B belong to rutile TiO_2 phase. The grain size of $0.6BaMoO_4$–$0.4TiO_2$ ceramics lies in the range of 2–10 μm and for samples with H_3BO_3–CuO addition sintered at 850°C/2 h, the grain size is in the range of 0.5–2.5 μm, which is much smaller than that of the pure $0.6BaMoO_4$–$0.4TiO_2$ ceramics. This may be attributed to the fact that the H_3BO_3–CuO addition lowers the sintering temperature of $(1-x)BaMoO_4$–$xTiO_2$ ceramics and that the grains have not fully grown. From Fig. 2(d), clear silver particles can be observed, which confirms that Ag does not react with $(1-x)BaMoO_4$–$xTiO_2$ composites combined with the XRD analysis.

Densities of $(1-x)BaMoO_4$–$xTiO_2$ ceramics as a function of x values are shown in Fig. 3(a). The theoretical densities of the compounds are calculated by the following formula:

$$\rho_{\text{theo}} = \frac{W_1 + W_2}{W_1/\rho_1 + W_2/\rho_2} \quad (2)$$

where, ρ_1 and ρ_2 are the theoretical densities of $BaMoO_4$ and TiO_2; W_1 and W_2 are the weight fractions of $BaMoO_4$ and TiO_2, respectively. The variation tendency of measured densities is in accordance with that of theoretical densities and the relative densities of the samples are all above 96%. The density of $0.662BaMoO_4$–$0.338TiO_2$ ceramics with H_3BO_3–CuO addition is shown in Table I. Figure 3(b) plots the microwave dielectric constant of $(1-x)BaMoO_4$–$xTiO_2$ composites. In composite ceramics, the dielectric constant is determined by the permittivity, volume fraction, and the complex form of the component material. Therefore, the theoretical permittivity (ε_{th}) of the $(1-x)BaMoO_4$–$xTiO_2$ compounds follows the Lichtenecker empirical logarithmic rule[15]:

$$\lg\varepsilon_{\text{th}} = y_1 \lg\varepsilon_1 + y_2 \lg\varepsilon_2 \quad (3)$$

where, ε_1 and ε_2 are permittivities of $BaMoO_4$ and TiO_2; y_1 and y_2 represent the volume fractions of $BaMoO_4$ and TiO_2 in the composites, respectively. As x value is the mole fraction of TiO_2, it is proportional to y_2 value, i.e., $x = (y_2 \times \rho_2/M_2)/(y_1 \times \rho_1/M_1 + y_2 \times \rho_2/M_2)$, where, M_1 and M_2 are the molar mass of $BaMoO_4$ and TiO_2, respectively. Figure 3(b) shows that the measured permittivity is consistent with the theoretical one. When x shifts from 0.2 to 0.66, the permittivity of the compound increases from 10.6 to 21.3.

The theoretical τ_f value is also obtained by the Lichtenecker logarithmic rule[15]:

$$\tau_f = y_1\tau_{f1} + y_2\tau_{f2} \quad (4)$$

where, τ_{f1} and τ_{f2} are the τ_f values of $BaMoO_4$ and TiO_2, respectively. There is a good agreement between the measured τ_f values and the theoretical ones as plotted in Fig. 3(c). When x varies from 0.2 to 0.66, the τ_f value shifts from −56.0 to 116.6 ppm/°C and the τ_f approaches near-zero value (−6.13 ppm/°C) when $x = 0.4$. Figure 3(d) presents the relationship between the $Q \times f$ values and the TiO_2 content. It can be seen that the $Q \times f$ values reach a maximum about 52 630 GHz at $x = 0.3$. When the mole fraction of TiO_2 rises, the sintering temperature of the $(1-x)BaMoO_4$–$xTiO_2$ composites increases due to the high sintering temperature of pure TiO_2. The $BaMoO_4$ phase changes to liquid phase and secondary recrystallization appears at higher temperature, which may result in the worsening of $Q \times f$ values when x exceeds 0.3.

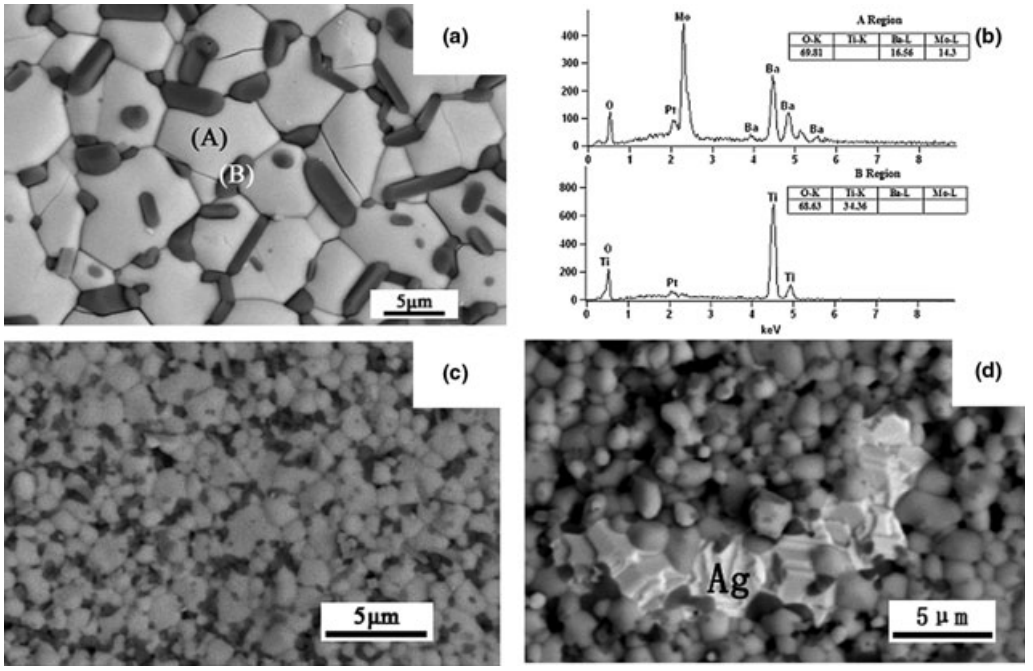

Fig. 2. Backscattered electron image (a) and EDS spectra (b) of the surfaces of $0.6BaMoO_4$-$0.4TiO_2$ compounds sintered at 1250°C/2h, backscattered electron images of (c) samples with H_3BO_3-CuO addition and (d) cofired samples with 20 wt% Ag sintered at 850°C/2h.

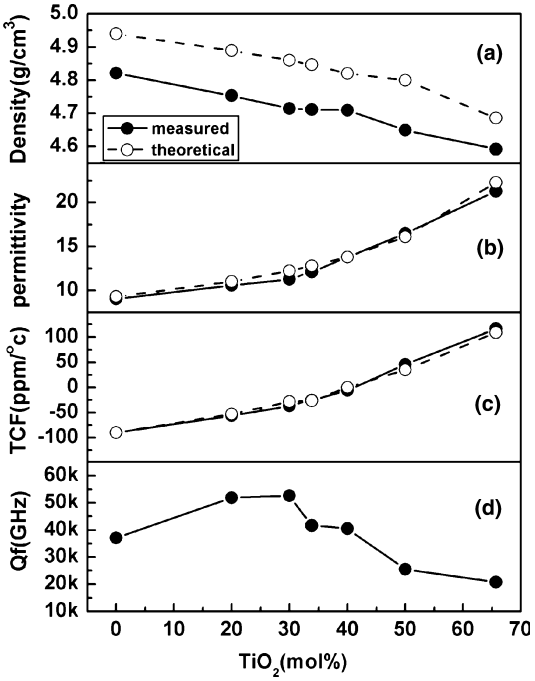

Fig. 3. (a) Densities, (b) microwave dielectric constant, (c) $Q \times f$ values, and (d) τ_f values of BMT ceramics as a function of x values.

Figure 4 shows the microwave dielectric properties of $0.6BaMoO_4$–$0.4TiO_2$ and $0.662BaMoO_4$–$0.338TiO_2$ with H_3BO_3–CuO addition as a function of sintering temperature. It is observed that the permittivity of $0.6BaMoO_4$–$0.4TiO_2$ is stable from 1175°C to 1275°C, and decreases sharply from 1275°C to 1300°C. It is probably caused by the $BaMoO_4$ phase change to liquid phase, and secondary recrystallization appears at high sintering temperature. The $0.6BaMoO_4$–$0.4TiO_2$ ceramics have a maximum $Q \times f$ value (40 500 GHz) at 1285°C and the $0.662BaMoO_4$–$0.338TiO_2$ with H_3BO_3–CuO addition possess a maximum $Q \times f$ value (48 360 GHz) at 875°C.

Figure 5 presents the IR reflectivity spectra of $(1-x)$ $BaMoO_4$–$xTiO_2$ composite ceramics with the lowest amount of TiO_2 and that have near-zero τ_f value. The spectra have been fitted according to the standard Lorentzian model[25] [Eq. (5)] and the Fresnel formula [Eq. (6)]:

$$\varepsilon^*(\omega) = \varepsilon_\infty + \sum_{j=1}^{n} \frac{\omega_{pj}^2}{\omega_{oj}^2 - \omega^2 - i\gamma_j\omega} \tag{5}$$

$$R(\omega) = \left| \frac{1 - \sqrt{\varepsilon^*(\omega)}}{1 + \sqrt{\varepsilon^*(\omega)}} \right|^2 \tag{6}$$

where, $\varepsilon^*(\omega)$ is complex dielectric function; ε_∞ is the dielectric constant caused by the electronic polarization at high frequencies; γ_j, ω_{oj}, and ω_{pj} are the damping factor, the

Table I. Densities and Microwave Dielectric Properties of $(1-x)BaMoO_4$–$xTiO_2$ Ceramics

	ST(°C)	Density (g/cm^3)	Permittivity	$Q \times f$ (GHz)	τ_f (ppm/°C)
$BaMoO_4$	900	4.821	9.0	37 110	−90.1
$0.8BaMoO_4 + 0.2TiO_2$	1275	4.754	10.6	51 840	−56.0
$0.7BaMoO_4 + 0.3TiO_2$	1285	4.715	11.3	52 630	−34.8
$0.662BaMoO_4 + 0.338TiO_2$	1285	4.712	12.1	41 620	−25.4
$0.6BaMoO_4 + 0.4TiO_2$	1285	4.710	13.8	40 500	−6.13
$0.5BaMoO_4 + 0.5TiO_2$	1285	4.649	16.5	25 520	+45.9
$0.34BaMoO_4 + 0.66TiO_2$	1300	4.592	21.3	20 705	+119.6
$0.662BaMoO_4 + 0.338TiO_2$ + BCu	875	4.625	14.0	48 360	+13.9

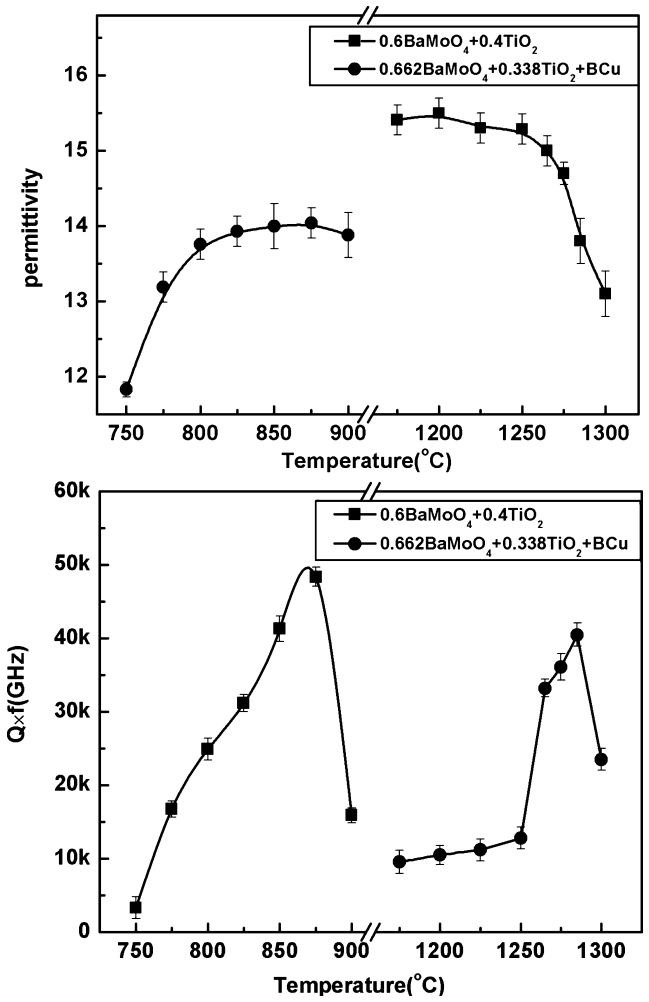

Fig. 4. Microwave dielectric properties of $0.6BaMoO_4$–$0.4TiO_2$ and $0.662BaMoO_4$–$0.338TiO_2$ with H_3BO_3–CuO addition as a function of sintering temperature.

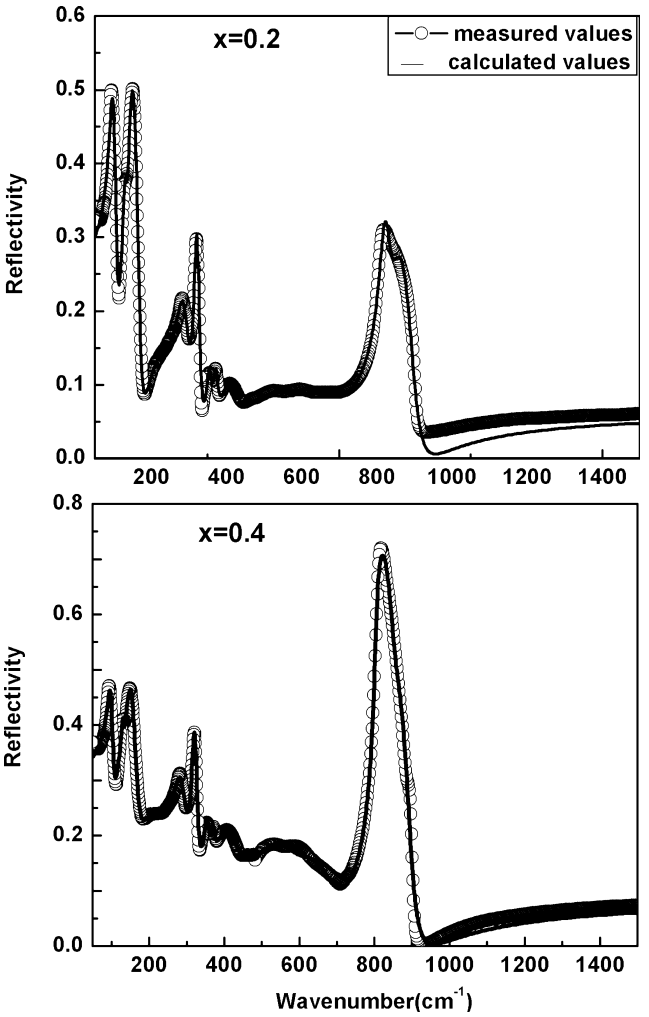

Fig. 5. Infrared reflectivity spectra of the $(1-x)BaMoO_4$–$xTiO_2$ composite ceramics.

Table II. Mode Parameters of a Lorentzian Fit in $(1-x)BaMoO_4$–$xTiO_2$ Ceramics

	x = 0.2 ε_∞ = 2.77				x = 0.4 ε_∞ = 3.31			
Mod	ω_{oj}	ω_{pj}	γ_j	$\Delta\varepsilon_j$	ω_{oj}	ω_{pj}	γ_j	$\Delta\varepsilon_j$
1	95.42	168.91	15.68	3.13	97.66	147	14.54	2.27
2	130.01	89.41	10.48	0.47	130.91	59.81	6.23	0.21
3	143.6	179.53	18.23	1.56	147.97	234.86	25.2	2.52
4	235.14	180.96	93.68	0.59	223.43	299.68	121.45	1.8
5	284.29	184.04	37.08	0.42	283.01	228.44	37.9	0.65
6	318.5	134.46	11.87	0.18	318.94	168.77	12.07	0.28
7	354.91	70.43	13.54	0.04	353.88	110.25	17.79	0.1
8	371.96	75.97	14.49	0.04	371.21	66.62	11.28	0.03
9	413.65	174.17	61.73	0.18	410.54	317.3	85.81	0.6
10	552.81	329.98	202.91	0.36	549.1	479.7	160.72	0.76
11	670.13	246.35	134.89	0.14	650.55	394.99	140.85	0.37
12	817.41	374.13	28.7	0.21	803.53	541.45	14.84	0.45
13	848.83	332.87	56.23	0.15	855.8	116.23	47.24	0.02

transverse frequency, and oscillator strength of the j-th Lorentz oscillator, respectively; n is the number of transverse phonon modes; and $R(\omega)$ is the IR reflectivity.

The $BaMoO_4$ has a tetragonal scheelite structure with symmetry C_{4h}^6 at room temperature. The optical phonon modes are described as follows[24]:

$$\Gamma = 3A_g + 5B_g + 5E_g + 5A_u + 3B_u + 5E_u \quad (7)$$

where, A_g, B_g, and E_g are Raman active; $4A_u$ and $4E_u$ can be only observed in IR spectra; B_u is silent mode; the left $1A_u$ and $1E_u$ are acoustic vibrations. There are 15 vibration modes in rutile TiO_2 among which $1A_u$ and $3E_u$ (E_u is two-fold degenerate) are IR active.[19,20] In this study, 13 reflection bands are identifiable. Among the vibration modes analyzed above, six peaks belong to rutile TiO_2 and seven peaks belong to scheelite $BaMoO_4$. Table II lists the fitted-mode

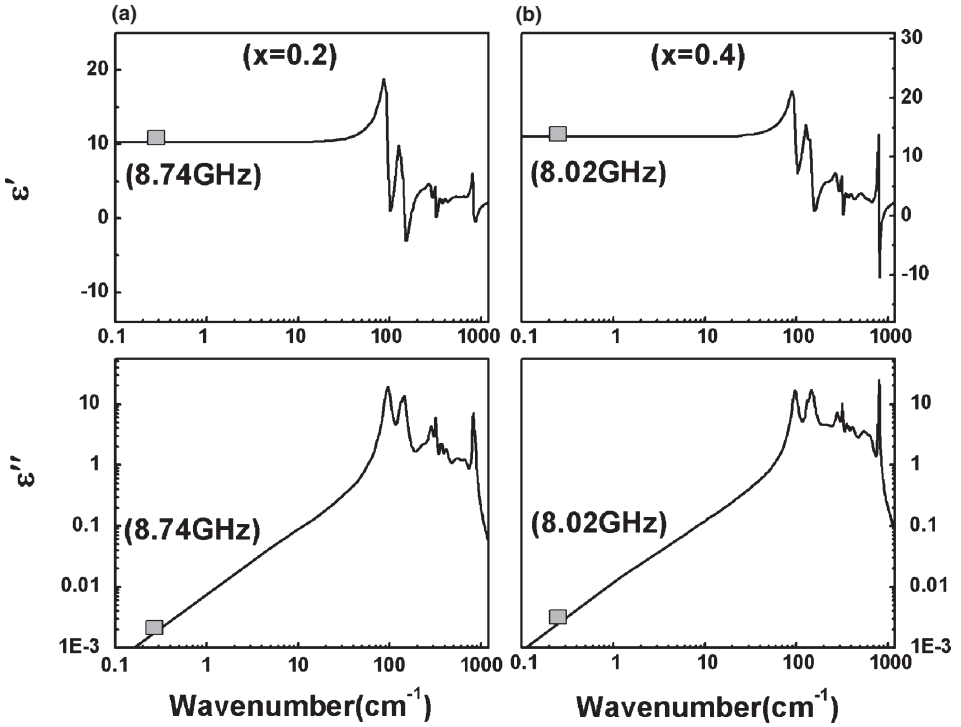

Fig. 6. The real and imaginary parts of the dielectric function of $(1-x)BaMoO_4$–$xTiO_2$ ceramics with (a) $x = 0.2$ and (b) $x = 0.4$.

parameters. The measured reflectivity spectra match well with the fitted ones. The fitted vibration bands of $BaMoO_4$ are at 97–100, 147–151, 284–287, 321–323, 371–373, 807–823, 841–856 cm^{-1} and the others belong to TiO_2. It is seen that the intensity of the reflectivity of TiO_2 increases and most modes of TiO_2 are more damped when x varies from 0.2 to 0.4 as shown in Fig. 5 and in Table II. This result indicates that $BaMoO_4$ coexists with TiO_2 and the contribution of TiO_2 to vibration rises when x increases.

The IR reflectivity data are transformed to complex dielectric data by the Kramers–Kroning relationship as plotted in Fig. 6. Compared with Table II, it is seen that vibration model 1 and model 3 make the most contribution to ε. Extrapolation of ε' from the IR spectra down to MW range shows that the measured permittivity corresponds with the calculated one which demonstrates that the MW dielectric constant of $(1-x)BaMoO_4$–$xTiO_2$ composite is caused mostly by the polar optical phonons.[26] The IR dielectric loss is mainly caused by intrinsic processes. Consequently, the ε'' extrapolated from the IR spectra should be slightly lower than the measured MW dielectric loss. From Fig. 6(b), it is seen that a good agreement between the measured and calculated ε'' is obtained which indicates that the intrinsic losses are the main MW dielectric losses of $(1-x)BaMoO_4$–$x TiO_2$.

IV. Conclusion

A new series of composite MW dielectric materials of $(1-x)$ $BaMoO_4$–$xTiO_2$ were prepared via the solid-state reaction method. The X-ray diffraction analysis indicates that scheelite $BaMoO_4$ and rutile TiO_2 phase coexist with each other and both of them do not react with silver (Ag). When the mole fraction of TiO_2 (x value) rises from 0 to 0.66, the MW dielectric properties varies as follows: $\varepsilon_r = 9.0$–21.3, $Q \times f =$ 20 705–52 630 GHz, and $\tau_f = -90.1$ to +13.9 ppm/°C. The measured MW dielectric losses are in consistent with the calculated ε'' obtained from IR spectra. With H_3BO_3–CuO addition, a low-firing (below 900°C) and temperature stable microwave dielectric material ($x = 0.662$) has been obtained, with $\varepsilon_r = 14$, $Q \times f = 48\ 360$ GHz, and $\tau_f = +13.9$ ppm/°C.

Acknowledgments

The authors thank the administrators in IR beamline workstation of National Synchrotron Radiation Laboratory (NSRL) for their help in the IR measurement.

References

[1]M. T. Sebastian and H. Jantunen, "Low Loss Dielectric Materials for LTCC Applications: A Review," *Int. Mater. Rev.*, **53** [2] 57–90 (2008).
[2]M. Valant and D. Suvorov, "Chemical Compatibility between Silver Electrodes and Low-Firing Binary-Oxide Compounds: Conceptual Study," *J. Am. Ceram. Soc.*, **83** [11] 2721–9 (2000).
[3]A. K. Axelsson and N. M. Alford, "Bismuth Titanates Candidates for High Permittivity LTCC," *J. Eur. Ceram. Soc.*, **26** [10] 1933–6 (2006).
[4]D. Zhou, H. Wang, L. X. Pang, C. A. Randall, and X. Yao, "Bi_2O_3-MoO_3 Binary System: An Alternative Ultra Low Sintering Temperature Microwave Dielectric," *J. Am. Ceram. Soc.*, **92** [10] 2242–6 (2009).
[5]D. Zhou, C. Randall, H. Wang, L. X. Pang, and X. Yao, "Microwave Dielectric Ceramics in Li_2O-Bi_2O_3-MoO_3 System with Ultra-Low Sintering Temperatures," *J. Am. Ceram. Soc.*, **93** [4] 1096–100 (2010).
[6]G. K. Choi, J. R. Kim, S. H. Yoon, and K. S. Hong, "Microwave Dielectric Properties of Scheelite (A = Ca, Sr, Ba) and Wolframite (A = Mg, Zn, Mn) $AMoO_4$ Compounds," *J. Eur. Ceram. Soc.*, **27** [8] 3063–7 (2007).
[7]G. K. Choi, S. Y. Cho, J. S. An, and K. S. Hong, "Microwave Dielectric Properties and Sintering Behaviors of Scheelite Compound $CaMoO_4$," *J. Eur. Ceram. Soc.*, **26** [10–11] 2011–5 (2006).
[8]E. S. Kim, B. S. Chun, R. Freer, and R. J. Cernik, "Effects of Packing Fraction and Bond Valence on Microwave Dielectric Properties of $A^{2+}B^{6+}O_4$ (A^{2+}: Ca, Pb, Ba; B^{6+}: Mo, W) Ceramics," *J. Eur. Ceram. Soc.*, **30** [7] 1731–6 (2010).
[9]G. Subodh and M. T. Sebastian, "Glass-free $Zn_2Te_3O_8$ Microwave Ceramic for LTCC Applications," *J. Am. Ceram. Soc.*, **90** [7] 2266–8 (2007).
[10]C. L. Huang, J. J. Yang, and Y. P. Chang, "Dielectric Properties of Low Loss (1-x)$(Mg_{0.95}Zn_{0.05})TiO_3$-x$SrTiO_3$ Ceramic System at Microwave Frequency," *J. Am. Ceram. Soc.*, **90** [3] 858–62 (2007).
[11]C. L. Huang, T. J. Yang, and C. C. Huang, "Low Dielectric Loss Ceramics in the $ZnAl_2O_4$-TiO_2 System as a τ_f Compensator," *J. Am. Ceram. Soc.*, **92** [1] 119–24 (2009).
[12]D. W. Kim, K. H. Ko, D. K. Kwon, and K. S. Hong, "Origin of Microwave Dielectric Loss in $ZnNb_2O_6$-TiO_2," *J. Am. Ceram. Soc.*, **85** [5] 1169–72 (2002).
[13]A. Belous, O. Ovchar, and D. Durilin, "High-Q Microwave Dielectric Materials Based on the Spinel Mg_2TiO_4," *J. Am. Ceram. Soc.*, **89** [11] 3441–5 (2006).
[14]S. H. Yoon, G. K. Choi, D. W. Kim, S. Y. Cho, and K. S. Hong, "Mixture Behavior and Microwave Dielectric Properties of (1-x)$CaWO_4$-xTiO_2," *J. Eur. Ceram. Soc.*, **27** [8] 3087–91 (2007).
[15]L. X. Pang, H. Wang, D. Zhou, and X. Yao, "A New Temperature Stable Microwave Dielectric with Low-Firing Temperature in Bi_2MoO_6-TiO_2 System," *J. Alloy. Compd.*, **493** [1] 626–9 (2010).

[16]J. Guo, D. Zhou, H. Wang, and X. Yao, "Microwave dielectric properties of (1-x)$ZnMoO_4$-xTiO_2 composites ceramics," *J. Alloy. Compd.*, **509** [19] 5863–5 (2011).

[17]K. Wakino, M. Murata, and H. Tamura, "Far Infrared Reflection Spectra of Ba(Zn,Ta)O_3-$BaZrO_3$ Dielectric Resonator Material," *J. Am. Ceram. Soc.*, **69** [1] 34–7 (1986).

[18]H. Tamura, D. Sagala, and K. Wakino, "Lattice-Vibrations of Ba($Zn_{1/3}$ $Ta_{2/3}$)O_3 Crystal with Ordered Perovskite Structure," *Jpn. J. Appl. Phys. Part 1*, **25** [6] 787–91 (1986).

[19]S. P. S. Porto, P. A. Fleury, and T. C. Damen, "Raman Spectra of TiO_2, MgF, ZnF_2, FeF_2, and MnF_2," *Phys. Rev.*, **154** [2] 522–6 (1966).

[20]G. A. Samara and P. S. Peercy, "Pressure and Temperature Dependence of the Static Dielectric Constants and Raman Spectra of TiO_2 (Rutile)," *Phys. Rev. B*, **7** [3] 1131–48 (1973).

[21]W. G. Spitzer, R. C. Miller, D. A. Kleinman, and L. E. Howarth, "Far Infrared Dielectric Dispersion in $BaTiO_3$, $SrTiO_3$, and TiO_2," *Phys. Rev.*, **126** [5] 1710–21 (1962).

[22]J. C. Sczancoski, L. S. Cavalcante, N. L. Marana, R. O. da Silva, R. L. Tranquilin, M. R. Joya, P. S. Pizani, J. A. Varela, J. R. Sambrano, M. Siu Li, E. Longo, and J. Andrés, "Electronic Structure and Optical Properties of $BaMoO_4$ Powders," *Curr. Appl. Phys.*, **10** [2] 614–24 (2010).

[23]A. Phuruangrat, T. Thongtem, and S. Thongtem, "Barium Molybdate and Barium Tungstate Nanocrystals Synthesized by a Cyclic Microwave Irradiation," *J. Phys. Chem. Solids*, **70** [6] 955–9 (2009).

[24]T. T. Basiev, A. A. Sobol, Y. K. Voronko, and P. G. Zverev, "Spontaneous Raman Spectroscopy of Tungstate and Molybdate Crystals for Raman Lasers," *Opt. Mater.*, **15** [3] 205–16 (2000).

[25]H. L. Liu, H. I. Chen, Y. T. Tzeng, C. T. Chia, K. C. Hsu, C. C. Chi, C. B. Chang, K. C. Leou, and I. N. Lin, "Effect of SnO_2 Addition on the Dielectric Properties of $Ba_2Ti_9O_{20}$ Ceramics in the High-Frequency Regime," *J. Appl. Phys.*, **100** [9] 094104 (2006).

[26]J. Petzelt and S. Kamba, "Submillimetre and Infrared Response of Microwave Materials: Extrapolation to Microwave Properties," *Mater. Chem. Phys.*, **79** [2–3] 175–80 (2003). □